Modeling the Sublimation-Driven Atmosphere of Io with DSMC. A.C. Walker, D.B. Goldstein, C.H. Moore, P.L. Varghese, L.M. Trafton, B.D. Stewart, University of Texas at Austin (andrew.walker@mail.utexas.edu).

Introduction: In 1979 the primary Ionian dayside species, sulfur dioxide, was detected by the Voyager IR spectrometer (IRIS) [1]; however, the dominant mechanism (volcanic activity or sublimation from surface frost) of atmospheric production still remains in question. The local dayside SO_2 vertical column abundance varies between 10^{16} and 6×10^{17} cm^{-2}, depending on latitude and whether any surface frosts, volcanoes, or lava lakes are present. There have been several attempts to model Io's rarefied atmosphere as a continuum; this is a poor approximation at high altitudes and away from the subsolar region. We simulate the atmosphere with a non-continuum method and attempt to reconcile the results with observations.

Constraining Observations: In the last few years there have been many important observations which could help develop an understanding of the underlying physics. We concentrate on Lyman-α images which were used to map the dayside column densities on Io [2], disk-integrated observations of the 19.3 μm SO_2 band [3], surface temperature data from the Galileo photopolarimeter-radiometer (PPR) [4], and Galileo near-infrared mapping spectrometer (NIMS) data which were used to derive the fractional abundance of SO_2 surface frost [5].

Model: We present a fully three-dimensional model of Io's sublimation atmosphere computed using the DSMC method [6]. The atmospheric density is controlled by the local vapor pressure and local areal coverage of SO_2 surface frost. The gas densities span the range from highly collisional (near the peak surface frost temperature at low altitudes) to free molecular flow (at high altitudes and on the nightside). Previous models of Io's atmosphere have been either one-dimensional, in which only the vertical structure and temporal evolution are investigated, or two-dimensional, which are axi-symmetric about the subsolar point. Our model uses the DSMC method which is valid throughout the entire atmosphere. Our three-dimensional simulation is able to model asymmetries in atmospheric parameters such as density, temperature, and flow velocity due to planetary rotation and an inhomogeneous frost distribution.

The atmosphere is most sensitive to the surface frost temperature distribution, T_{frost}, due to the exponential dependence of vapor pressures on this parameter. T_{frost} is matched to the nightside cooling rate of surface temperature data from the Galileo PPR [4].

Results: The effects on Io's atmosphere of planetary rotation, heating due to plasma bombardment, inhomogeneous surface frost, SO_2 residence time on rock, subsolar temperature, and volcanic plumes are examined. The subsolar temperature, T_{ss}, is parameterized to be either 120 K or 115 K.

Overall flow features. Circumplanetary flow develops as the high vapor pressure region near the peak T_{frost} pushes gas toward the low vapor pressure region on and near the nightside. The vapor pressure drops rapidly near the terminator as the surface cools. The flow is forced to be nearly parallel to the surface by the high day-to-night pressure gradient. The winds are not directly away from the region of origin because the inhomogeneous surface frost alters the pressure field leading to a slight curvature of the streamtraces. Weak irregular flows up to 50 m/s do develop where strong frost gradients occur. These weak flows are more visible on the nightside where the surface temperature is nearly constant and the flow is nearly free molecular. The pressure gradient between the warmest point on Io and the terminator is strong enough to drive the flow supersonic. When the supersonic gas slows to subsonic speeds on and near the nightside, a C-shaped shock is formed.

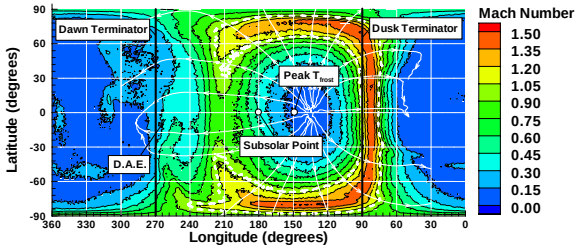

Figure 1 – Color contours of the Mach number at an altitude of 30 km as a function of latitude and longitude. Streamtraces tracking the flow are in white and the sonic line is shown by a dashed white line.

Temperatures. The translational temperature, T_{trans}, exhibits an interesting structure due to the plasma heating for the baseline atmosphere. Near the surface, T_{trans} closely tracks T_{frost} because the SO_2 gas is nearly in thermodynamic equilibrium with the surface. Below 1 km altitude, at the location of the peak T_{frost}, the sublimated SO_2 gas cools by infra-red and microwave radiation (corresponding to vibrational and rotational transitions) and expands as it moves upward and spreads laterally [7]. T_{trans} then increases with altitude above 1 km due to the plasma heating, despite the gas continuing to expand and radiate. For these two reasons, the lower atmosphere has a volume of cold gas bracketed above and below by warmer gas. Above 1 km, T_{trans} becomes dependent upon the plasma energy

flux reaching that location. The column is much thicker above the peak T_{frost} region, so the plasma energy flux is absorbed by the upper atmosphere (above 1 km), leaving the lower atmosphere unaffected. The altitude at which the plasma is completely absorbed by the atmospheric column decreases away from the region of peak T_{frost} (because the column decreases). T_{trans} also increases in the rarefied C-shaped shock due to compressive heating.

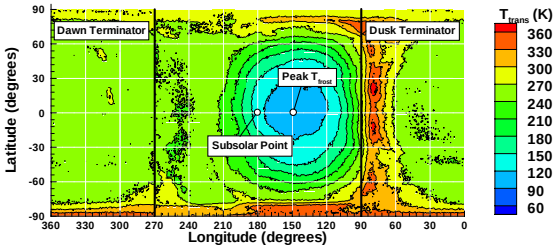

Figure 2 – Color contours of T_{trans} at an altitude of 3 km as a function of latitude and longitude.

The rotational temperature, T_{rot}, is maintained in equilibrium with T_{trans} if the collision rate is sufficiently high; departures from thermal equilibrium occur because the collision rate drops as the density decreases with altitude. T_{rot} is in equilibrium with T_{trans} at altitudes below 5 km on the nightside and below 50 km on the dayside, corresponding to a gas density greater than ~6.5×10^{8} cm^{-3}. At higher altitudes, T_{trans} continues to increase due to plasma energy input whereas T_{rot} warms more slowly as the energy input from collisions and plasma is not sufficient to balance the energy loss from microwave radiation.

The vibrational temperature of the ν_2 vibrational mode of SO_2, T_{vib}, is only in equilibrium with T_{trans} very near the surface; everywhere away from the surface T_{vib} is highly nonequilibrium. This is because the only two mechanisms which can yield a vibrationally excited SO_2 molecule in our current model are collisions and sublimation from the surface (since the departing molecule is assumed to be in thermal equilibrium with the surface) and the vibrational excitation rate by collisions is much slower than the de-excitation rate by radiative emission everywhere in the atmosphere.

Number and Column Densities. The vertical column density is found to be predominantly controlled by the surface temperature (exponential dependence), with the surface frost coverage having a comparatively small effect (proportional), and winds having an even lesser effect. The vertical column density also departs from hydrostatic equilibrium at the location of the dawn atmospheric enhancement where the atmosphere is not only sustained by sublimation from the frost, but additionally by the rapid desorption of all the SO_2 gas which condensed onto rock during the night.

The *peak* equatorial vertical column density is 3.9×10^{16} cm^{-2} and the subsolar vertical column density is 2.95×10^{16} cm^{-2} with error estimates of $\pm5\times10^{14}$ cm^{-2} on all vertical column densities. Feaga *et al.* (2009) determined the dayside peak vertical column density to be 5.0×10^{16} cm^{-2} on the anti-Jovian hemisphere, 4.2×10^{16} cm^{-2} at the anti-Jovian point, and 1.5×10^{16} cm^{-2} at the sub-Jovian point. The agreement is relatively good with our simulations and could be improved by increasing our assumed subsolar temperature of the surface to 116 K or 117 K. It is, however, important to note that the simulation vertical column densities do not include the column from active volcanoes. Column densities inferred from disk-averaged 19.3 μm observations [3] are 1.5×10^{17} cm^{-2} at 180º W and 1.5×10^{16} cm^{-2} at 300º W which are higher on the anti-Jovian hemisphere and lower on the sub-Jovian hemisphere than our simulations.

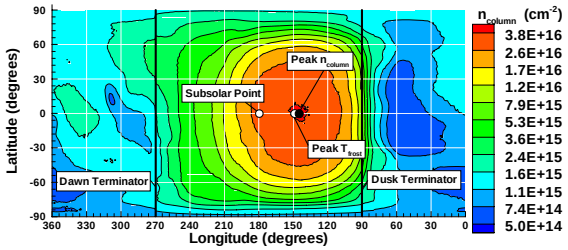

Figure 3 – Color and line contours of the column density as a function of latitude and longitude.

A striking feature of the Lyman-α inferred column densities is the sharp fall off in column near ±45º latitude [2,8]. The latitudinal variation in our modeled column densities exhibits a much smaller decrease at mid-latitudes than those inferred from the Lyman-α observations. The column density variation in our model is directly related to T_{frost} which at the peak T_{frost} essentially follows a $\cos^{1/4}(\psi)$ latitudinal variation.

References: [1] Pearl, J., et al. (1979) *Nature* **280**, 755-758. [2] Feaga, L., et al. (2009) *Icarus* **201**, 570-584. [3] Spencer, J., et al. (2005) *Icarus* **176**, 283-304. [4] Rathbun, J., et al. (2004) *Icarus* **169**, 127-139. [5] Douté, S., et al. (2001) *Icarus* **149**, 107-132. [6] Bird, G. (1994) *Molecular gas dynamics and the direct simulation of gas flows.* Oxford press [7] Moore, C., et al. (2009) *Icarus* **201**, 585-597. [8] Strobel, D. and Wolven, B., (2001) *Ast. & Sp. Sci.* **277**, 271-287.